Mater Renew Sustain Energy (2015) 4:8
DOI 10.1007/s40243-015-0050-0

ORIGINAL PAPER

An experimental investigation of mesoporous MgO as a potential pre-combustion CO_2 sorbent

Sushant Kumar[1] · Surendra K. Saxena[1] · Vadym Drozd[1] · Andriy Durygin[1]

Received: 10 May 2014 / Accepted: 8 May 2015 / Published online: 22 May 2015

Abstract We examined the CO_2 capture capacity of mesoporous MgO (325 mesh size, surface area = 95.08 ± 1.5 m^2/g) as a potential pre-combustion CO_2 sorbent. Our results show that 96.96 % of MgO was converted to $MgCO_3$ at 350 °C and 10 bars CO_2 pressure. The sorbent could be completely regenerated at 550 °C under argon flow. The sorption rate parameters such as surface area and pore size were investigated.

Keywords Capture capacity · Mesoporous · Pre-combustion · Sorbent · Surface area · Pore size

Introduction

Fossil fuel accounts for the world's major energy supply and its use is anticipated to be continued throughout the 21st century [1]. The use of fossil fuel is always accompanied with a vast emission of CO_2. The anthropogenic CO_2 emissions upset the natural carbon cycle leading to an increased atmospheric CO_2 concentration. No one can deny that there is an urgent need to develop methods for CO_2 mitigation.

Currently, a large focus is devoted on capturing CO_2 from coal-fired power plant flue streams, which continues to be the major CO_2 contributor [2].There are three main technological approaches for CO_2 capture- post-, oxy- and pre-combustion. Post-combustion systems capture CO_2 from N_2-rich flue gas stream, produced by burning fossil fuel in air. Oxy-combustion uses pure stream of O_2, instead of air, to combust coal and thus produces CO_2-rich gas stream. On the other hand, pre-combustion systems are designed mainly to remove CO_2 from the syngas ($CO + H_2$) prior to its combustion for power production [3]. Under pre-combustion conditions, after the water–gas shift reactor ($CO + H_2O \rightarrow CO_2 + H_2$), the gas stream mainly consists of CO_2, H_2O and H_2. The partial CO_2 pressure for pre-combustion capture conditions is around 20–30 bar and the temperature is between 250 and 450 °C [4].

Both the physical and chemical solvents can be used for pre-combustion CO_2 capture. Unlike chemical solvent, physical solvent (such as Selexol and Rectisol) selectively absorbs CO_2 without forming any chemical bonds. Thus, the physical solvent requires relatively less regeneration energy as compared to that of chemical solvent [5]. However, these physical solvent-based processes suffer severe disadvantages: (1) lose pressure during regeneration step, and (2) require a low operating temperature. Therefore, syngas needs to be cooled prior to CO_2 absorption step to attain a relatively low operating temperature. After CO_2 absorption, the remaining hydrogen gas stream requires to be reheated to the gas turbine inlet temperature. However, chemical solvents have the advantage of high mass transfer driving force into solution and better acid gas selectivity. Also, chemical solvents can be used in processes that utilize thermal swing regeneration and generate the CO_2 at elevated pressure [6]. But chemical solvents increase the energy and cost penalty and thus are downgraded as a future CO_2 sorbent [7].

Electronic supplementary material The online version of this article (doi:10.1007/s40243-015-0050-0) contains supplementary material, which is available to authorized users.

✉ Sushant Kumar
skuma002@fiu.edu

[1] Center for the Study of Matter at Extreme Conditions, College of Engineering and Computing, Florida International University, Miami, FL 33199, USA

Currently, the focus is to develop advanced physical and chemical solvent systems that have the potential to provide significant improvements in both cost and performance as compared to the Selexol and Rectisol for pre-combustion CO_2 capture. The challenges are to modify regeneration conditions to recover the CO_2 at a higher pressure, improve selectivity to reduce H_2 losses, and develop a solvent that has a high CO_2 loading at a higher temperature, which would increase integrated gasification combined cycle (IGCC) efficiency. In the same line, another vital task is to develop a new sorbent which could be highly efficient for pre-combustion capture conditions. Consequently, the US Department of Energy (DOE) performed the thermodynamic modeling activities that included screening analyses for a number of different metal oxides, zirconates, silicates and titanates under various operating conditions to identify new solid sorbents for pre-combustion CO_2 capture. About 18 sorbents were modeled and finally seven candidates are chosen—magnesium oxide (MgO), calcium oxide (CaO), lithium zirconate (Li_2ZrO_3), calcium zirconate ($CaZrO_3$), barium zirconate ($BaZrO_3$), barium titanate ($BaTiO_3$) and barium silicate ($BaSiO_3$) for further investigations [8]. Among these solid sorbents, MgO and CaO are attractive because of their easy accessibility and favorable thermodynamic properties [9].

The alkaline earth metal oxides (such as CaO and MgO) combine with CO_2 to form thermodynamically stable carbonates. Metal carbonates, when heated, liberate pure stream of CO_2 gas and regenerate the oxides. Eventually, the generated pure CO_2 gas can either be sequestered underground or used for enhanced oil recovery [10]. CaO are abundant and thus relatively easily accessible than MgO. However, CaO as CO_2 sorbent suffers severe major drawbacks and a detailed discussion can be found elsewhere [11]. It is a fact that regeneration of oxides needs a lot of energy [12]. MgO and $Mg(OH)_2$ are known to be better candidates than CaO for CO_2 capture applications due to their low regeneration energy requirement and low operating temperature [13]. Thus, MgO (periclase), although occurs only rarely as an oxide, we choose it here for our study. One should note that MgO when recycled between naturally occurring magnesite or dolomite can cause relatively lesser energy or carbon emission penalty [14].

The CO_2 absorption capacity of MgO was studied as a function of particle size, surface area, temperature, pressure, support and concentration of water vapor. The CO_2 uptake capacity on different MgO sorbents at different conditions is listed in Table 1. Most of the experiments are restricted to low temperature and ambient or low pressure condition. Hence, the reported sorption capacities of CO_2 on MgO are not very high. However, the sorbents which can operate in the range of 300–350 °C would be ideal for the use in IGCC applications. Therefore, we study the CO_2 capture capacity of MgO in the relatively high temperature and pressure condition of 300–375 °C and 10–50 bars, respectively.

Experimental procedure

The reaction

$$MgO(s) + CO_2(g) \leftrightarrow MgCO_3(s)$$

was studied experimentally. The carbonation reaction was performed in a closed system which permits us to efficiently maintain high temperature and pressure for a long period of time. The decomposition reaction of carbonate was examined using Thermo gravimetric Analysis (TGA) technique.

About 0.2 g of 325-mesh-sized magnesium oxide (delivered by Alfa Aesar) was put inside a closed cylindrical vessel (1.25″ long and 0.35″ internal diameter). About 0.1 ml of water was also introduced on the vessel walls. Chemically pure CO_2 gas (Airgas) was passed into this system. Before experiments, CO_2 gas was flushed three times to ensure a pure CO_2 atmosphere inside the reactor. The reaction was performed for 30 min at a desired temperature and pressure condition. Once the reaction completed, the system was air-cooled. The product was then ground using mortar and pestle. The powder particle was again put back for another reaction at the same experimental condition. This cycle was repeated until no increment in weight of the product was observed.

Thermo gravimetric analysis (TGA) of the product was done using TGA 2950 Thermo gravimetric analyzer. The samples (10 mg) were heated under argon purge, at a heating rate of 10 °C/min to a final temperature of 800 °C. The TGA provides continuous measurements of the sample weight as a function of time and temperature. The amount of formation of $MgCO_3$ was analyzed by the percent loss in weight of the sample while heating up to 800 °C in an argon atmosphere.

The product characterization was performed using X-ray powder diffraction method. Bruker GADDS/D8 is equipped with Apex Smart CCD Detector and direct-drive rotating anode. The MacSci rotating anode (Molybdenum) operates with a 50 kV generator and 20 mA current. X-ray beam size can vary from 50 to 300 μm. The usual collection time is 1200 s.

An isothermal gas adsorption was employed to measure internal surface areas of the powder particles. Micromeritics Tristar II 3020 (surface area and porosimetry analyzer instrument) was used with N_2 as adsorptive gas at 77 K (liquid nitrogen bath). The samples were first degassed under 300 °C with a N_2 gas flow for 1 h to remove

Table 1 CO_2 uptake capacity of MgO obtained from the literature

	Sorbent	Gas stream	Carbonation temperature (°C)	Pressure (bar) or, flow rate	Particle Size	Regeneration temperature (°C)	CO_2 capture capacity (mmol/g) conversion, %	References
1	MgO	Pure CO_2	50–1000	100 mL/min (flow rate)	–	–	0.99	[15]
2	MgO/Al_2O_3 (10 wt. % MgO)	(13 v % H_2O, 13 v % CO_2)	30, 150	1	(20–40) mesh size	350	1.36	[16]
3	MgO	(11 v % H_2O, 1 v % CO_2)	50–100	0.01	–	150–400	1.05	[17]
4	K_2CO_3/MgO	(11 v % H_2O, 1 v % CO_2)	50–100	–	–	150–400	2.98	[17]
5	MgO	330/660 ppm in air	0, 100	0.2	–	–	0.64, 0.43	[18, 19]
6	MgO/MCM-41	Pure CO_2	25	1	–	–	1.06	[20]
7	Mesoporous MgO	Pure CO_2	25, 100	1	–	–	1.82, 2.27	[21]
8	Nonporous MgO	Pure CO_2	25	1	–	–	0.45	[21]
9	MgO–ZrO_2	Pure CO_2	30, 150	1	–	–	1.15,1.01	[22, 23]
10	MgO (31.7 wt%)/Al_2O_3 (22.4 wt%)	Pure CO_2	20, 200, 300	1	–	–	0.13, 0.24, 0.5	[24]
11	MgO (33.8 wt%)/ Al_2O_3 (20.8 wt%)	Pure CO_2	20, 200, 300	1	–	–	0.08, 0.12, 0.5	[24]
12	K_2CO_3/MgO/Al_2O_3	Flue gas	60	1	–	480	2.49	[25]
13	K_2CO_3/MgO	(9 v % H_2O, 1 v % CO_2)	60	40 mL/min (flow rate)	–	400	2.7	[26]
14	MgO nanocrystal	Flue gas	60	25sccm (flow rate)	5 nm	60–600	6.4	[27]
15	MgO	Pure CO_2	350	1.33, 3.33	–	–	0.089, 0.091	[28]
16	MgO	Pure CO_2	300–500	9–36	<44 μm	–	70–80 % (~200 min)	[29]
17	MgO	Pure CO_2	–	20–40	<44 μm	–	100 % (~120 min)	[30]

the moisture and other adsorbed gases before analysis. The internal surface area was calculated using the Brunauer–Emmett–Teller (BET) method. The pore volume was also calculated from the adsorbed nitrogen after complete pore condensation ($P/P_0 = 0.9925$) using the ratio of the densities of liquid and gaseous nitrogen. The pore size was calculated using the Barrett–Joyner–Halenda (BJH) method.

Results and discussion

Figure 1 confirms the formation of $MgCO_3$ at different temperatures and CO_2 pressures. MgO, $Mg(OH)_2$, $MgO{\cdot}2MgCO_3$ and $MgCO_3$ were identified conventionally by their corresponding Joint Committee Powder Diffraction Standard (JCPDS) card number 79-0612,82-2345,31-0804 and 86-2345, respectively.

One of the vital factors in gas–solid carbonation reaction is the presence of water and there have been numerous observations where water acts as a catalyst [31–34]. Therefore, we have also used water (0.1 ml) for the MgO–CO_2 reaction. In absence of water, no CO_2 was absorbed at these conditions due to the kinetic limitations. The CO_2 sorption capacity of MgO increases significantly in the presence of water vapor. Under humid condition, MgO rapidly locks CO_2 in the form of $MgCO_3$. Recently, Fagerlund et al. [29] proposed the reaction mechanism for MgO carbonation in the presence of steam:

$$MgO + H_2O \leftrightarrow MgO \cdot H_2O^*$$

$$MgO \cdot H_2O^* + CO_2 \leftrightarrow MgCO_3 + H_2O$$

$$MgO + CO_2 \leftrightarrow MgCO_3$$

Figure 2 depicts the adsorption/absorption model for MgO–CO_2–H_2O reaction. Based on the previous work, it could be reasonable to corroborate that water vapor surrounds MgO particles where CO_2 reacts to form CO_3^{2-} ions and H^+ ions [34–36]. Free Mg^{+2} ions could further react with the CO_3^{2-} ions to form $MgCO_3$. However, $MgCO_3$ forms an impervious layer around unreacted MgO particles and hinders the further diffusion of CO_2 molecules.

Here, we used mortar and pestle to grind the product. As mentioned earlier, we conducted each experiment for 30 min and ground the sample after that. Grinding helps in scrubbing off the outer nonporous layer of $MgCO_3$. And we performed grinding until we noticed no change in product weight after subsequent experiments. In general, after 3–4 cycles, we observed no change in the weight of product. It is certain that such intermittent grinding step is limited to the laboratory and cannot be seen as an industrial operation. Therefore, it is recommended to have an aggregative fluidization regime for a fluidized bed reactor while scaling up MgO–CO_2 reaction. Also, increasing the amount of water vapor cannot lead to the complete carbonate conversion of MgO. Thus, in addition to the amount of steam, surface properties of MgO (such as surface area, particle size, porosity) are also very crucial parameters for the carbonation process.

The thermal analysis curve does not show any significant differences in amounts of carbonate in the high-pressure (50 bars) experiments. We obtained almost similar TGA plots and XRD patterns for different temperatures 300–375 °C and 50 bars CO_2 pressure. However, the experiment performed at 300 °C and 10 bars did indicate that the product was not simply $MgCO_3$. The X-ray diffraction

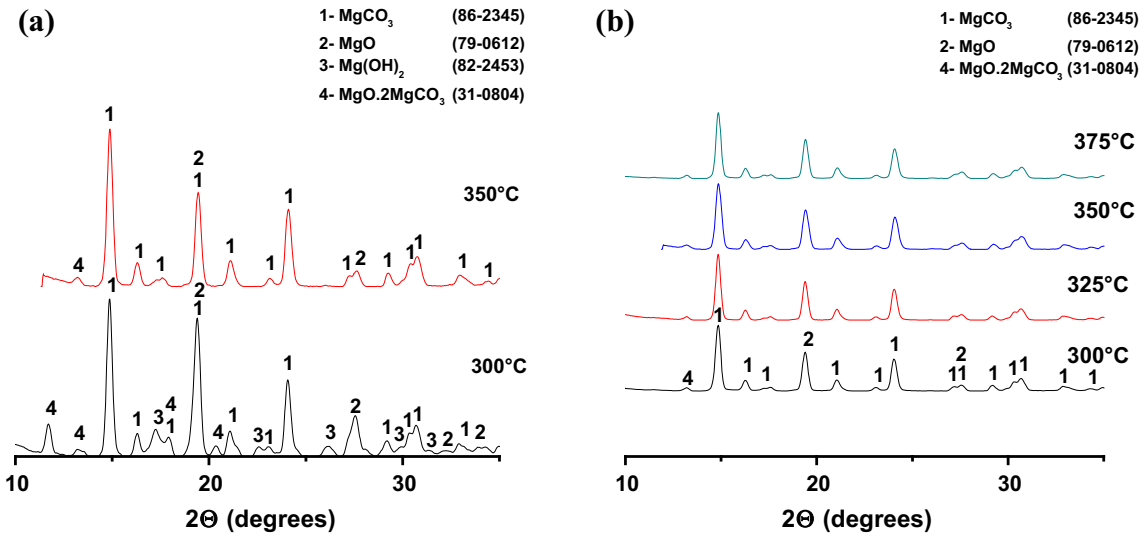

Fig. 1 XRD patterns for $MgCO_3$ formation after reaction at various temperatures and CO_2 pressure of **a** 10 bars and **b** 50 bars

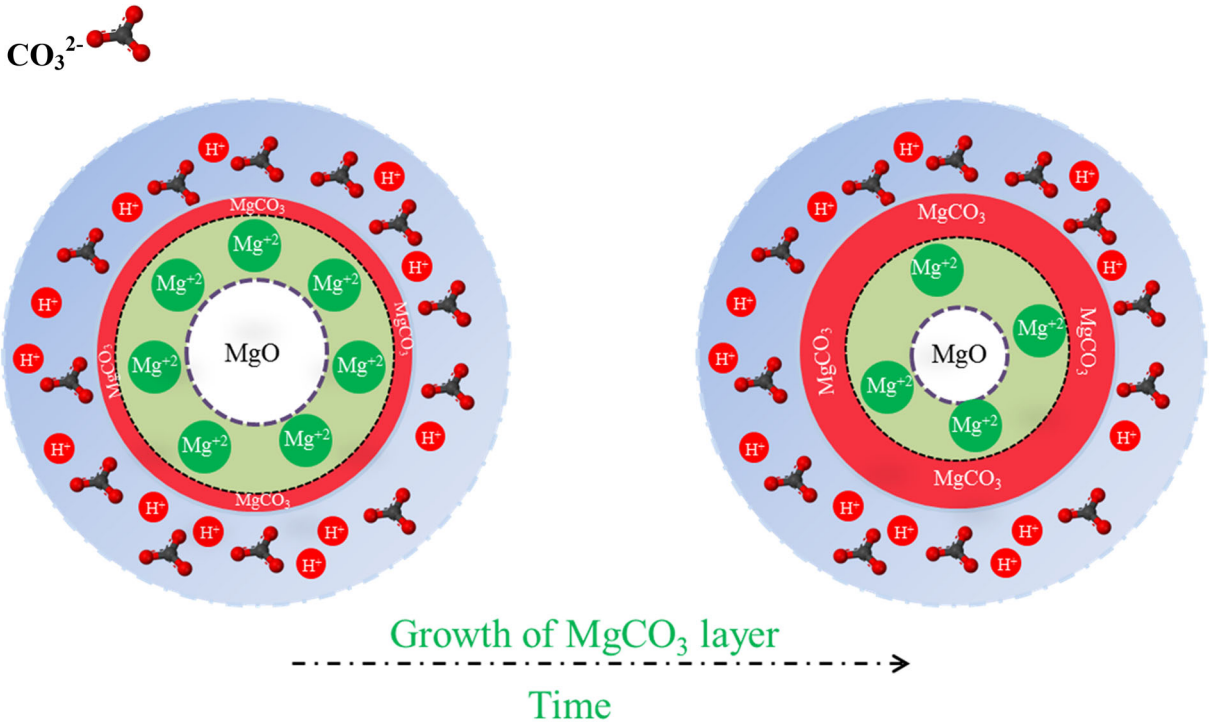

Fig. 2 The adsorption/absorption model for MgO–CO_2–H_2O reaction

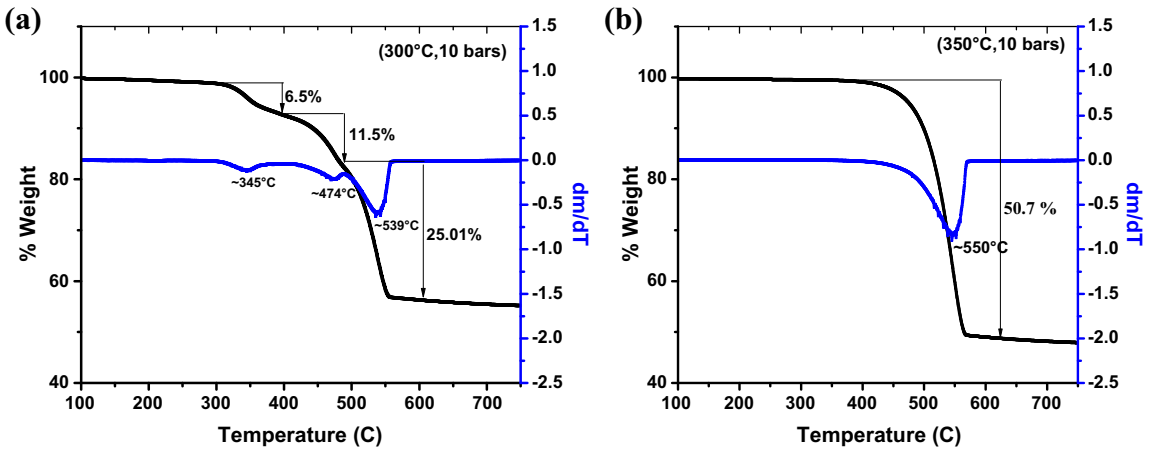

Fig. 3 DTG plots for product at **a** 300 °C and 10 bars and **b** 350 °C and 10 bars

pattern in Fig. 1a confirms the presence of Mg $(OH)_2$ and relatively high amount of $MgO{\cdot}2MgCO_3$ at 300 °C and 10 bars. DTG curve (Fig. 3a) also evidences the similar situation. The two peaks around 350 and 475 °C were attributed to the losses of water of crystallization and hydroxyl water, respectively. However, another peak at 550 °C corresponds to the complete decomposition of $MgCO_3$. But at a temperature and pressure of 350 °C and 10 bars, respectively, only $MgCO_3$ was formed. This is evidenced by both DTG (Fig. 3b) and X-ray diffraction analysis (Fig. 1a).

The steps to calculate % conversion of MgO to $MgCO_3$ is explained in supplementary section [S1]. A conversion of 30.54 and 96.96 % for MgO to $MgCO_3$ was observed at 300 and 350 °C, respectively. Here, we observed the formation of relatively high amount of oxymagnesite ($MgO{\cdot}2MgCO_3$) at 300 °C and 10 bars. It can be easily calculated that the CO_2 capture capacity of oxymagnesite is about two-third that of $MgCO_3$. Hence, formation of oxymagnesite can markedly reduce the overall uptake of CO_2 by MgO particles. However, it can be observed from X-ray patterns (Fig. 1) that at higher

Table 2 Surface properties of MgO particles before and after carbonation reaction 350 °C, 10 bars

Sample	Surface area (m^2/g)	Pore volume (cm^3/g)	Pore size (nm)	SA/PV(10^6 m^{-1})
As-received MgO	95.08 ± 1.5	0.22	9.09	439.59
After reaction at (350 °C, 10 bars)	4.15 ± 0.05	0.01	16.25	246.15

temperature or pressure, the formation of oxymagnesite is suppressed.

In the same line, recent study reveals that oxymagnesite forms as an intermediate during the thermal decomposition of hydrated magnesium carbonate [37]. Moreover, oxymagnesite can also be formed as a product of reaction between Mg (OH) $_2$ and CO_2 in anhydrous synthesis [29] and/or solid-state reaction of MgO and CO_2 using steam [38]. In this regard, Duan et al. [13] calculated the phase diagram of MgO–Mg(OH) $_2$–$MgCO_3$, which suggests that the transition temperature for direct conversion of $MgCO_3$ to $Mg(OH)_2$ increases with increase in P_{H2O}. Here, when temperature increases from 300 to 350 °C, partial pressure of water also increases and consequently transition temperature also increased. At 300 °C, a relatively less amount of MgO transforms to its carbonates. This can be attributed to a possible high conversion of $MgCO_3$ to Mg(OH) $_2$, which is in agreement with the phase diagram. Moreover, a significant formation of oxymagnesite at 300 °C and 10 bars also leads to a less direct conversion of MgO to $MgCO_3$. Thus, it can be deduced that a high amount of oxymagnesite forms at a low partial pressure of water. Therefore, the reaction mechanism is changed to:

$$MgO + CO_2 \leftrightarrow MgCO_3$$

$$MgO + 2MgCO_3 \leftrightarrow MgO \cdot 2MgCO_3$$

$$MgO \cdot 2MgCO_3 + CO_2 \leftrightarrow 3MgCO_3$$

Moreover, at 50 bars of CO_2 pressure and a temperature of 300 °C, MgO has the highest yield of 98.54 %. At high temperatures (300–375 °C) but constant pressure (50 bars), we observe a slight but continuous decrease in the absorption of CO_2, which is in congruence with previously reported results [30]. It is well known that at low temperature, the physisorption process dominates but at elevated temperature CO_2 chemisorbs on MgO and thus CO_2 uptake capacity gradually starts decreasing.

CO_2-uptake capacity of a metal oxide is primarily dominated by the factors such as surface area, pore volume, pore functionality and pore size [28]. BET surface area measurement, pore volume and average pore sizes presented in Table 2 indicates the significant role of CO_2 to influence the particle structure. As received, 325 mesh size mesoporous MgO has a pore size of 9.09 nm and a high surface area (95.08 ± 1.5 m^2/g). Figure 4 illustrates that the N_2 adsorption–desorption isotherm curves for as-received MgO follows Type IV isotherms (as per IUPAC classification); typical for mesoporous substances [39]. Also, the hysteresis pattern is H3 (following IUPAC classification) indicating the presence of slit-like pores. After capture of CO_2 at 350 °C and 10 bars, surface area dramatically decreased to (4.15 ± 0.05) m^2/g. The ratio of surface area to pore volume is also reduced by almost half and results in high diffusion paths. The significant decrease in surface area attributes to the basicity of mesoporous MgO. The mesoporous MgO is highly basic with well-ordered pores to hold high CO_2 at both lower and higher temperatures. It is well known that porous materials allow molecules to pass through their pore aperture for storage, separation or conversion [36]. MgO with a fine particle size (<44 μm) has a high content of mesopores, which leads to good mass transfer properties during the absorption process. The mechanism for metal oxide reaction with CO_2 gas has been discussed a lot [40–43]. CO_2 molecules diffuse through the pores of mesoporous MgO and the present large active sites hold these CO_2 molecules [19]. The trapped CO_2 molecules further react to form $MgCO_3$.

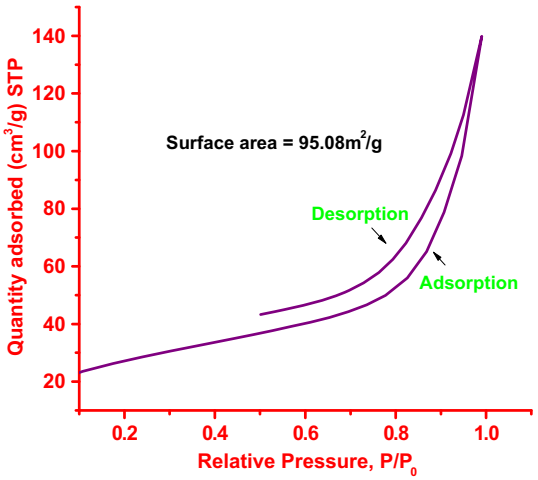

Fig. 4 N_2 adsorption–desorption isotherm of as-received MgO

It can be observed from Table 2 that at 350 °C and 10 bars, 96.96 % of MgO was converted to $MgCO_3$ and almost all the pores have been utilized after reaction with CO_2 molecules. Henceforth, almost no CO_2 molecules could have diffused further in the pores. Noticeably, pore size increased to 16.25 nm. Thus, it is apparent that the porosity of MgO particles plays a very vital role for CO_2 uptake.

Previously, Beruto et al. has reported a very low CO_2 absorption capacity of MgO in absence of water vapor [27]. An uptake capacity of 0.089 and 0.091 mmol CO_2/g MgO was observed at 350 °C in 1.33 and 3.33 bars of CO_2, respectively. Thus, it was concluded that there is a high activation energy barrier to MgO recarbonation. On the contrary, Feng et al. [14] heated the sorbent (MgO) to 1000 °C in pure CO_2 and noted a low but almost constant (for 8 cycles) absorption capacity of 0.99 mmol CO_2/g MgO. Thus, unlike CaO-based sorbents, MgO does not show a fast decline in their CO_2 capture capacity over a large number of carbonation–calcination cycles. Bhagiyalakshmi et al. [20] synthesized basic mesoporous MgO (surface area of 250 m^2/g) using mesoporous carbon obtained from SBA-15 and obtained a maximum CO_2 adsorption of 2.27 mmol CO_2/g at 100 °C and nearly 1.81 mmol CO_2/g at 25 °C for a feed flow rate of 30 ml/min CO_2 gas (99.9 % purity). Therefore, it is evident that even for a relatively lower surface area (95 m^2/g compared to 250 m^2/g), MgO can have a better CO_2 uptake at a higher temperature (here, 300–375 °C) and higher CO_2 pressure (10–50 bars). Recently, Fagerlund et al. [28] reported a very high % conversion of MgO to $MgCO_3$ under high temperature and pressure conditions. However, MgO showed a slow conversion rate (50 % for ~7 h) for the condition [P_{CO2} (~18–19 bar), P_{H2O} (~1–2 bar) and 300–350 °C] which can be suitable for pre-combustion capture process. The reason could be the deposition of impervious carbonate layer on the surface of MgO which does not allow CO_2 molecules to further diffuse in the pores. Therefore, continuous removal of these nonporous layers of carbonates is needed. As mentioned earlier, we recommend to have an aggregative fluidization regime for a fluidized bed reactor while scaling up MgO–CO_2 reaction.

In summary, we demonstrate the increase in uptake of CO_2 by mesoporous MgO at high temperature and pressure in the humid environment. We observed the significant role of temperature, pressure, water vapor and porosity of the sorbent on the improvement of the CO_2 absorption capacity of mesoporous MgO.

Conclusion

MgO is a promising candidate for pre-combustion CO_2 capture due to their stable absorption capacity of CO_2, adequate mechanical strength, high attrition resistance and good regenerability. We observed a 96.96 % of MgO conversion to $MgCO_3$ at 350 °C and 10 bars CO_2 pressure. Moreover, CO_2 uptake capacity of MgO can be increased by performing the reaction in the presence of slight humid environment and scrubbing off the outer non-porous layer of $MgCO_3$. We also demonstrate that MgO has a low regeneration temperature (550 °C) and stable CO_2 capture capacity over wide range of temperature and pressure. Interestingly, the present study also illustrate that a high amount of oxymagnesite forms at a low partial pressure of water.

References

1. Kumar, S.: Clean hydrogen production methods, Springer Briefs in energy. Springer, New York (2015)
2. Merkel, T.C., Lin, H., Wei, X., Baker, R.: Power plant post-combustion carbon dioxide capture: an opportunity for membranes. J. Membr. Sci. **359**, 126–139 (2010)
3. Davison, J.: Performance and costs of power plants with capture and storage of CO_2. Energy **32**, 1163–1176 (2007)
4. Burton, B.P., Dupin, N., Fries, S.G., Grimvall, G., Fernández Guillermet, A., Miodownik, P., Oats, W. A., Vinograd, V., Z. Metallkd **92**, 514 (2001)
5. Miller, B., Tillman, D.: Combustion engineering issues for solid fuel systems. pp. 449–451. Elsevier (2008)
6. DOE/NETL: Carbon dioxide capture and storage RD&D roadmap, (2010)
7. Yu, C.H., Huang, C.H., Tan, C.S.: A review of CO_2 capture by absorption and adsorption. Aerosol Air Qual. Res. **12**, 745–769 (2012)
8. Evaluation of Dry Sorbent Technology; Presentation at the 2010 NETL CO_2 Capture Technology Meeting, Pittsburgh, PA, September 13–17, 2010
9. Kumar, S., Saxena, S.K.: A comparative study of CO_2 sorption properties for different oxides. Mater. Renew. Sustain. Energy **3**, 30 (2014)
10. Benson, S.M., Cole, D.R.: CO_2 sequestration in deep sedimentary formations. Elements **4**, 325–331 (2008)
11. Gruene, P., Belova, A.G., Yegulalp, T.M., Farrauto, R.J., Castaldi, M.J.: Dispersed calcium oxide as a Reversible and efficient CO_2-sorbent at intermediate temperatures. Ind. Eng. Chem. Res. **50**, 4042–4049 (2011)
12. Rackley, S.: Carbon capture and storage. Elsevier, Burlington (2010)
13. Duan, Y., Sorescu, D.C.: CO_2 capture properties of alkaline earth metal oxides and hydroxides: a combined density functional theory and lattice phonon dynamics study. J. Chem. Phys. **133**, 074508–074511 (2010)
14. Feng, B., An, H., Tan, E.: Screening of CO_2 adsorbing materials for zero emission power generation systems. Energy Fuels **21**, 426–434 (2007)
15. Li, L., Wen, X., Fu, X., Wang, F., Zhao, N., Xiao, F., Wei, W., Sun, Y.: MgO/Al_2O_3 sorbent for CO_2 capture. Energy Fuels **24**, 5773–5780 (2010)
16. Lee, S.C., Chae, H.J., Lee, S.J., Choi, B.Y., Yi, C.K., Lee, J.B., Ryu, C.K., Kim, J.C.: Development of regenerable MgO-based sorbent promoted with K_2CO_3 for CO_2 capture at low temperatures. Environ. Sci. Technol. **42**, 2436–2471 (2008)
17. Ward, S.M., Braslaw, J., Gealer, R.L.: Carbon dioxide sorption studies on magnesium oxide. Thermochim. Acta **64**, 107–114 (1983)

18. Choi, S., Drese, J.H., Jones, C.W.: Adsorbent materials for carbon dioxide capture from large anthropogenic point sources. Chemsuschem **2**, 796–854 (2009)
19. Fu, X., Zhao, N., Li, J., Xiao, F., Wei, W., Sun, Y.: Carbon dioxide capture by MgO-modified MCM-41 materials. Adsorpt. Sci. Technol. **27**, 593–601 (2009)
20. Bhagiyalakshmi, M., Lee, J.Y., Jang, H.T.: Synthesis of mesoporous magnesium oxide: its application to CO_2 chemisorption. Int. J. Greenhouse Gas Control **4**, 51–56 (2010)
21. Liu, S., Zhang, X., Li, J., Zhao, N., Wei, W., Sun, Y.: Preparation and application of stabilized mesoporous MgO–ZrO_2 solid base. Catal. Commun. **9**, 1527–1532 (2008)
22. Li, B., Wen, X., Zhao, N., Wang, X.Z., Wei, W., Sun, Y., Ren, Z.H., Wang, Z.J.: Preparation of high stability MgO–ZrO_2 solid base and its high temperature CO_2 capture properties. J. Fuel Chem. Technol. **38**, 473–477 (2010)
23. Yong, Z., Mata, V., Rodrigues, A.E.: Adsorption of carbon dioxide onto hydrotalcite-like compounds (HTlcs) at high temperatures. Ind. Eng. Chem. Res. **40**, 204–209 (2001)
24. Li, L., Li, Y., Wen, X., Wang, F., Zhao, N., Xiao, F., Wei, W., Sun, Y.: CO_2 capture over K_2CO_3/MgO/Al_2O_3 dry sorbent in a fluidized bed. Energy Fuels **25**, 3835–3842 (2011)
25. Lee, S.C., Choi, B.Y., Lee, T.J., Ryu, C.K., Soo, Y.S., Kim, J.C.: CO_2 absorption and regeneration of alkali metal-based solid sorbents. Catal. Today **111**, 385–390 (2006)
26. Ruminski, A.M., Jeon, K.J., Urban, J.J.: Size-dependent CO_2 capture in chemically synthesized magnesium oxide nanocrystals. J. Mater. Chem. **21**, 11486–11491 (2011)
27. Beruto, D., Botter, R., Searcy, A.W.: Thermodynamics of two, two–dimensional phases formed by CO_2 chemisorption on MgO. J. Phys. Chem. **91**, 3578–3581 (1987)
28. Lu, W., Yuan, D., Sculley, J., Zhao, D., Krishna, R., Zhou, H.C.: Sulfonate-grafted porous polymer networks for preferential CO_2 adsorption at low pressure. J. Am. Chem. Soc. **133**, 18126–18129 (2011)
29. Fagerlund, J., Highfield, J., Zevenhoven, R.: Kinetics studies on wet and dry gas-solid carbonation of MgO and $Mg(OH)_2$ for CO_2 sequestration. RSC Adv. **2**, 10380–10393 (2012)
30. Highfield, J., Bu, J., Fagerlund, J., Zevenhoven, R.: ICCDU-XI (2011)
31. Butt, D.P., Pile, S.P., Park, Y., Vaidya, R., Lackner, K.S., Wendt, C.H., Nomura, K.: Report LA-UR-98-7631 (1998)
32. Hassanzadeh, A., Abbasian, J.: Regenerable MgO-based sorbents for high-temperature CO_2 removal from syngas: 1. sorbent development, evaluation, and reaction modeling. Fuel **89**, 1287–1297 (2010)
33. Kato, Y., Yamashita, N., Kobayashi, K., Yoshizawa, Y.: Kinetic study of the hydration of magnesium oxide for a chemical heat pump. Appl. Therm. Eng. **16**, 853–862 (1996)
34. Liu, C., Shih, S.: Kinetics of the reaction of iron blast furnace slag/hydrated lime sorbents with SO2 at low temperatures: effects of the presence of CO_2, O_2, and NO_X. Ind. Eng. Chem. Res. **48**, 8335–8340 (2009)
35. Zevenhoven, R., Teir, S., Eloneva, S.: Heat optimisation of a staged gas-solid mineral carbonation process for long-term CO_2 storage. Energy **33**, 362–370 (2008)
36. Zevenhoven, R., Eloneva, S., Teir, S.: A study on MgO-based mineral carbonation kinetics using pressurized thermogravimetric analysis. GHGT-8, Norway, (2006)
37. Frykstrand, S., Stietzel, C., Forsgren, J., Angstrom, J., Potin, V., Stromme, M.: Synthesis, electron microscopy and X-ray characterization of oxymagnesite, $MgO{\cdot}2MgCO_3$, formed from amorphous magnesium carbonate. CrystEngComm **16**, 10837–10844 (2014)
38. Fagerlund, J., Nduagu, E., Romao, I., Zevenhoven, R.: CO_2 fixation using magnesium silicate minerals part 1: process description and performance. Energy **41**, 184–191 (2012)
39. Li, R., Chen, G., Dong, G., Sun, X.: Controllable synthesis of nanostructured TiO2 by CTAB-assisted hydrothermal route. New J. Chem. **38**, 4684–4689 (2014)
40. Deng, H., Grunder, S., Cordova, K.E., Valente, C., Furukawa, H., Hmadeh, M., Gándara, F., Whalley, A.C., Liu, Z., Asahina, S., Kazumori, H., O'Keeffe, M., Terasaki, O., Stoddart, F.J., Yaghi, O.M.: Large-pore apertures in a series of metal-organic frameworks. Science **336**, 1018–1023 (2012)
41. Bhatia, S.K., Perlmutter, D.D.: Effect of the product layer on the kinetics of the CO_2 –Lime Reaction. AIChE J. **29**, 79–86 (1983)
42. Butt, D.P., Lackner, K.S., Wendt, C.H., Conzone, S.D., Kung, H., Lu, Y.C., Bremser, J.K.: Kinetics of thermal dehydroxylation and carbonation of magnesium hydroxide. J. Am. Ceram. Soc. **79**, 1892–1898 (1996)
43. Kumar, S.: The effect of elevated pressure, temperature and particle morphology on the carbon dioxide capture using zinc oxide. J. CO_2 Util. **8**, 60–66 (2014)